Received: 15 July 2021 | Accepted: 1 October 2021

DOI: 10.1111/bpa.13030

Brain Pathology

LETTER TO THE EDITOR

Distinct subcortical tau burden: The tau pallido-claustral ratio separates progressive supranuclear palsy and corticobasal degeneration

Abstract

Neuropathological diagnosis of progressive supranuclear palsy (PSP) and corticobasal degeneration (CBD) requires interpretation of tau morphology based on extensive brain sampling. Here we report subcortical tau burden is sufficient to distinguish PSP and CBD, regardless of the tau morphology. The tau pallido-claustral ratio is a promising diagnostic indicator for PSP and CBD.

As the two tauopathies commonly presented with Parkinsonism, progressive supranuclear palsy (PSP) and corticobasal degeneration (CBD) overlap both clinically and pathologically [1]. Immunohistochemistry using antibodies for phosphorylated tau or specific tau isoform (4R) can identify a variety of tau immunoreactive lesions in both neurons and glia. Neuronal tau that aggregates in both PSP and CBD include pretangles, neurofibrillary tangles, dystrophic neurites, and threads. Tufted astrocytes, thorn-shaped astrocytes, astrocytic plaques, and coiled bodies are the glial tau-immunopositive lesions seen in these two diseases [2]. Tufted astrocytes are considered characteristic for PSP, whereas the astrocytic plaques are pathognomonic for CBD. The neuropathological diagnosis of PSP and CBD is based on distinguishing the tau-positive lesion morphology and tau pathology distribution of these two diseases.

Koga et al. have recently proposed a machine learning-based decision tree classifier to distinguish PSP and CBD. Without considering the morphological features of astrocytic tau lesions, the proposed classifier was able to distinguish PSP and CBD with high accuracy [3]. However, this study and many of the previously published series were conducted based on a semiquantitative, 4-point scale system for tau-pathology (none/absent = 0, mild = 1, moderate = 2, severe = 3) [3, 4]. Although the assessment and scoring were performed by experienced neuropathologist(s), this manual scoring system is subjective and often prone to inter-observer variability. Moreover, most of these studies were conducted based on research-orientated brain biobanks, with extensive sampling of many different brain regions. However, this is not always possible for pathologists who work in institutions where strict tissue retention policies are in place.

With the recent development of digital pathology image analysis, automated unbiased whole-slide quantification of immunohistochemistry becomes possible. Here, we apply this approach by using the digital image analysis software *QuPath* to quantify total tau-disease burden, based on limited sampling of selected subcortical brain regions. We aim to establish a simplified protocol to distinguish between PSP and CBD.

This study was approved by the Western University Research Ethics Board (HSREB 113886). All cases were investigated at the London Health Sciences Centre (LHSC) under formal autopsy consent. We performed a retrospective case search at the Department of Pathology and Laboratory Medicine at LHSC for the period of 2000 to 2019, based on the primary neuropathological diagnosis. We included 28 Neuropathology confirmed tauopathy cases, including 10 PSP, 8 CBD, and 10 Alzheimer's disease (AD) (Table S1). The AD assessment was performed according to the National Institute on Aging–Alzheimer's Association guidelines [5]. There were 5 AD-high level (AD-H) and 5 AD-intermediate level (AD-I) cases. None of the AD patients had parkinsonian symptoms or other movement impairments.

Formalin fixed brains were sampled and prepared using routine procedures as described previously [6]. Hematoxylin, Eosin, and Luxol fast blue (HE/LFB) stained sections were used to visually identify and outline the areas of interest (AOI) (Figure 1A). Immunohistochemical staining for phospho-Tau (Ser202/Thr205) (1: 4000, mouse monoclonal, clone AT8,

Invitrogen, Cat # ENMN1020) was performed using Dako Autostainer Link 48 and counterstained with hematoxylin. All slides were scanned at 40X magnification with Aperio XT system (Leica Biosystems). The digitalized slides were analyzed with the open source software *QuPath* (version 0.2.0-m11, https://qupath.github.io/) [7]. We used the tau-positive pixel counts (PPC) as a surrogate for tau-disease burden. The immunopositive pixels were counted using a color deconvolution algorithm, with the pixel size set as 0.25 μm and a "positive" threshold of 0.3. Nearly all tau immunopositive pathology was detected and analyzed with this setting (Figure 1B,C). Tau quantification was represented by the positive pixel ratio (positive pixel %), calculated as: positive pixel % = (positive pixel count)/(total pixel count of the AOI) × 100%. The scanned whole slide was reviewed by a neuropathologist to ensure annotation accuracy, and to exclude any staining artifact. Eighteen subcortical AOIs were examined, including striatum (putamen and caudate), external and internal globus pallidus (GPe, GPi), claustrum, subthalamic nucleus (STN), thalamus [anterior, medial dorsal (MD), intralaminar, ventral lateral (VL) and zona incerta (ZI)], midbrain [tectum, tegmentum, substantia nigra (SN)], pons (tegmentum and basis pontis), cerebellar dentate, anterior and posterior limbs of the internal capsule.

All statistical tests were conducted with R (Version 1.2.5033) [8]. One-way ANOVA and student t-test were used to compare the differences among groups of patients, with a p-value <0.05 taken as statistically significant. The unsupervised hierarchical clustering method using dissimilarity distance and average linkage was invoked to partition the patients based on the tau-disease burden. The logistic model is employed to construct a predictive model for the type of diseases and the receiver operating characteristic (ROC) curve is used to assess the prediction. Youden's index was used to determine the appropriate cut-off values for the patient classes [9]. Figures were generated on GraphPad Prism (Version 9.1.1) and Tableau (Version 2020.3).

We first compared the regional tau-disease burden among these four groups. Figure 1B,C illustrated various tau-pathology morphologies, which were detected and analyzed as total tau-burden. The quantification of tau pathology was summarized in Figure 1D. As expected, CBD demonstrated an overall most severe tau pathology in nearly all AOIs. Despite its wide connection to the cortical and subcortical structures, claustrum has received very little attention in pathology literatures. Interestingly, there was a significantly lower claustral tau burden in patients with PSP compared with CBD and AD-H. This trend was similarly observed in the striatum. In contrast, both PSP and CBD cases showed higher tau burden in the globus pallidus (GPe and Gpi) and STN when compared with AD-H. When the thalamus was divided into subgroups, the anterior nuclei were more involved in AD-H, whereas the MD, VL, and intralaminar nuclei showed more tau burden in patients with CBD. In the brainstem regions, both PSP and CBD had a higher tau burden in the SN and midbrain tegmentum than AD-H. The SN is also moderately involved in AD-H. Not surprisingly, AD-I has the lowest tau-burden in all AOIs (data not shown).

We then performed unsupervised hierarchical clustering based on the tau-disease burden of 10 PSP, 8 CBD, and 10 AD cases. PSP and CBD cases were clearly separated into the top and bottom clusters respectively, while all AD cases were placed in the middle (Figure 2A). Case 68 (pathological diagnosis of PSP) was clustered within the AD-I group, because of the overall low level of tau burden. Case 31 (pathological diagnosis of CBD) was placed within the AD-H cluster as a result of the absence of STN reading. There was no overlap between PSP and CBD cases.

As extensive brain sampling is not always possible for many nonresearch-oriented pathology laboratories and medical examiner's offices, we were interested in locating the "high yield" brain regions, or one "core" brain slice. The coronal hemispheric section at the level of STN contains many key structures pertaining to movement functions (Figure 1A). After we created a neuroanatomical heatmap of tau burden severity based on this "core" brain slice, distinct tau distribution patterns became clear (Figure 2B). CBD had an overall high tau burden across all regions. PSP showed a higher tau pathology along the *pallido-nigro-luysian* axis. Tau accumulation in AD-H was largely restricted to the striatum, claustrum, anterior, and mediodorsal nuclei of the thalamus. AD-I had the lowest tau pathology in all regions.

To further simplify the diagnostic protocol, we decided to explore the possibility of a key predictor with a "cut-off value" to distinguish these conditions. We noticed a striking difference in the tau-burden ratio between globus pallidus and claustrum (tau-PC ratio) among PSP, CBD, and AD-H. CBD cases had similar tau burden in GP and claustrum and therefore the average tau-PC ratio is near 1.3. In contrast, the average tau-PC ratio was approaching 11 in PSP, but as low as 0.15 in AD-H (Figure 2B). A Youden index-based tau-PC ratio cut-off value of 1.5 was able to distinguish PSP from CBD with a near 100% positive predictive value (Figure S1).

In conclusion, using objective quantification by digital imaging analysis, we confirmed that regardless of the tau morphology, the severity and distribution pattern of the subcortical tau burden were sufficient to distinguish PSP, CBD, and AD. In part, we validated the decision tree proposed by Koga et al. [3]. Recognizing the differential tau burden in the striatum and claustrum is important for the diagnosis of PSP and CBD.

The claustrum was localized as the most sensitive and specific connectivity in new-onset Parkinsonism by lesion network mapping [10]. Here we provided pathological evidence that the claustral involvement was significantly different between PSP and CBD, the two most common tauopathies with Parkinsonism. Future studies

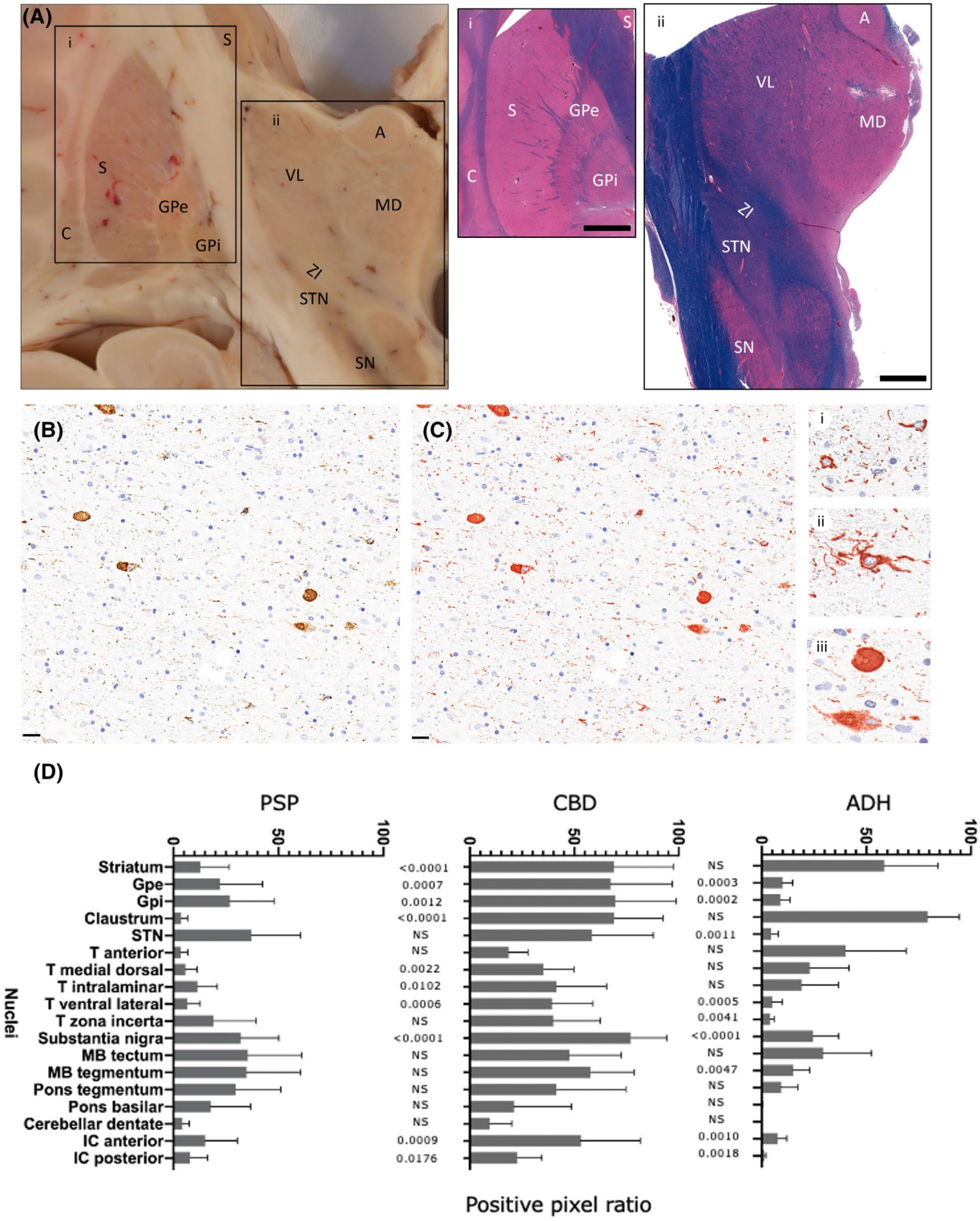

FIGURE 1 Representative images of areas of interest, tau immunopositive lesions, and QuPath analysis. (A) Coronal section of the left hemisphere at the level of subthalamic nucleus (case 04). Ten regions are annotated based on HE/LFB stain (Ai-ii). (B) tau immunohistochemistry stain highlights various tau-pathology morphologies (case 04, STN). (C) Positive immunolabeling detected by *QuPath* (red color overlay). Nearly all tau-pathology, including coiled bodies (i), tufted astrocyte (ii), neuronal pretangles, tangles, and small tau-positive threads (iii) are detected and included in tau-disease burden analysis by the *QuPath* algorithm. (D) Regional tau-disease burden in PSP, CBD, and AD-H. Scale bar in A = 3 mm; in B = 20 μm. A, thalamus anterior nucleus; C, claustrum; Gpe and GPi, external and internal globus pallidus; MD, thalamus medial dorsal nucleus; S, striatum (putamen and caudate); SN, substantia nigra; STN, subthalamic nucleus; VL, thalamus ventral lateral nucleus

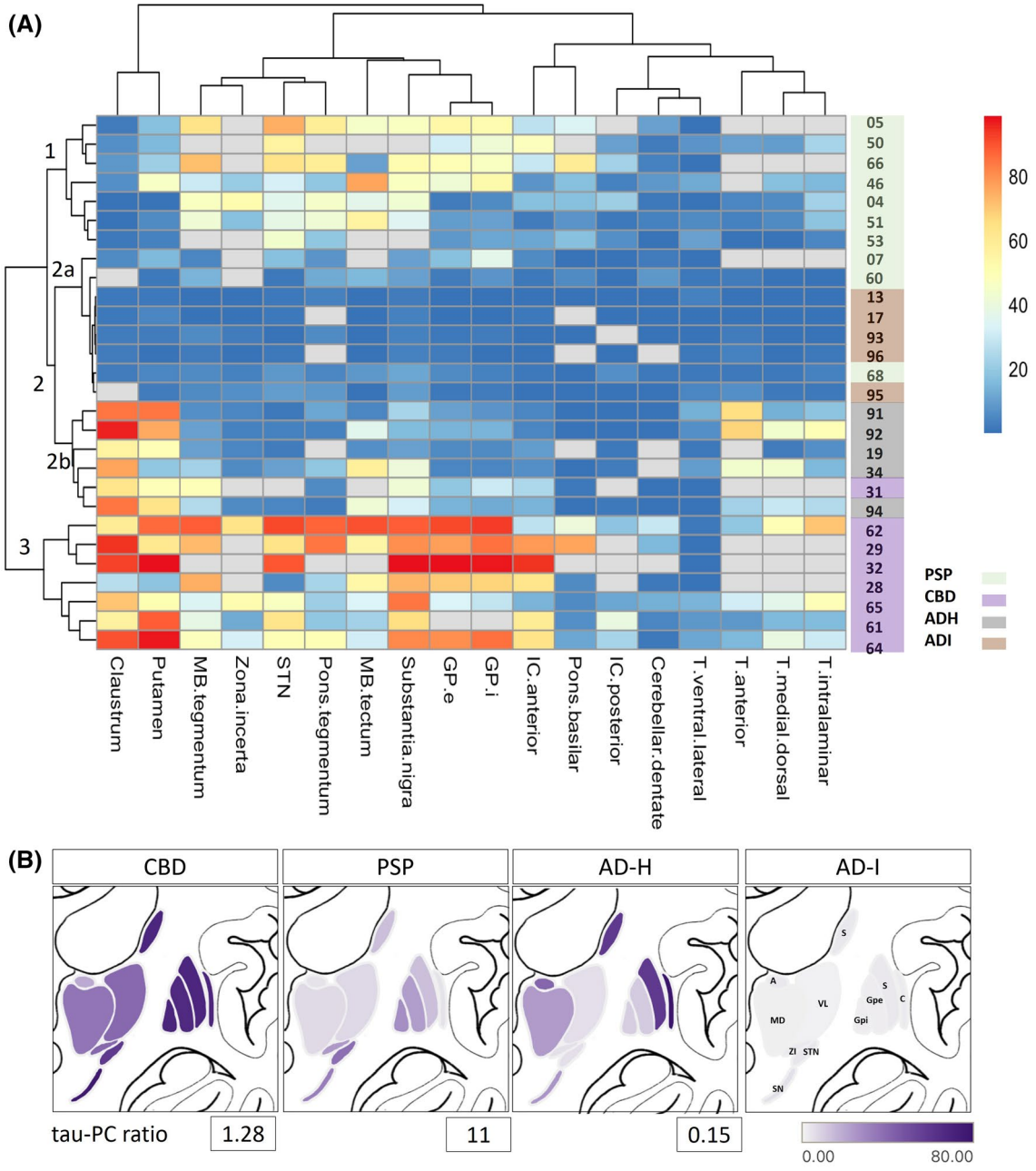

FIGURE 2 Hierarchical clustering and regional heatmap based on tau-disease burden. (A) Unsupervised hierarchical clustering based on the tau-disease burden of 10 PSP, 8 CBD, 5 AD-I, and 5 AD-H cases. Each brain region is represented in columns, and each case is represented in rows and colored coded with disease group. The severity of the tau burden is shown in a color scale, with red indicating the highest tau burden, blue indicating the lowest tau burden, and grey representing missing data. All CBD cases are clustered on the bottom, next to AD-H. All PSP cases are placed on the top. (B) A regional heatmap of tau burden severity is illustrated on the "core" brain slide. The severity of tau burden is shown in a color scale, with darker color reflecting higher severity. A distinct tau distribution pattern is shown. CBD has an overall high tau burden across all regions. PSP shows a higher tau pathology along the pallido-nigro-luysian axis. AD-H is largely restricted to the striatum, claustrum, anterior, and mediodorsal nuclei of the thalamus. The average tau pallido-claustral ratio (tau-PC ratio) is shown on the bottom of panel (B). A, thalamus anterior nucleus; C, claustrum; GPe and GPi, external and internal globus pallidus; MD, thalamus medial dorsal nucleus; S, striatum (putamen and caudate); SN, substantia nigra; STN, subthalamic nucleus; VL, thalamus ventral lateral nucleus

are needed to explore the mechanisms underlying these differences.

Neuropathological examination of potential PSP or CBD cases often requires extensive sampling of different brain regions. For non-research-based neuropathologists and forensic pathologists who work in institutions with strict tissue retention policies, whole brain retention is not always an option. In this study, we propose a simplified protocol. The coronal cerebral section at the level of the subthalamic nucleus

could serve as the "core" brain slice when examining suspected PSP or CBD cases. We also find the tau-PC ratio as a promising diagnostic criterion. As globus pallidus and claustrum are located close to each other and are often sampled together for microscopic examination, assessment of the tau-PC ratio should be easy to perform and be the first step of the decision tree when differentiating PSP and CBD. A case with a higher tau-PC ratio (>1.5) has a high possibility to be PSP. When slides digitalization and quantification are not readily available, experienced pathologists should be able to appreciate the distinct staining patterns by "eyeballing" the tau IHC slide. In essence, as shown in Figure 2B, when there is high tau-burden present in both globus pallidus and claustrum, it is likely a "CBD pattern." On the other hand, a "PSP pattern" will have a significantly lower tau burden in claustrum than the globus pallidus.

One major limitation of this study is the small sample size. A larger patient cohort is required to establish an optimal tau-PC ratio cut-off threshold and to validate the predictive value of this simplified diagnostic tool. Once external validity is proven by other neuropathology groups, a similar approach of tau-PC ratio could be developed for clinical diagnosis of PSP and CBD using neuroimaging such as PET with tau tracer.

KEYWORDS
claustrum, corticobasal degeneration, digital pathology, progressive supranuclear palsy, tauopathy

FUNDING INFORMATION
This research was conducted with the support of Western University Pathology Internal Funds for Academic Development (PIFAD) to QZ; the Western University Dean's Undergraduate Research Opportunity Program (DUROP) to CZ

ACKNOWLEDGMENTS
This research was conducted with the support of Western University Pathology Internal Funds for Academic Development (PIFAD) to QZ; the Western University Dean's Undergraduate Research Opportunity Program (DUROP) to CZ. The authors thank the staff of LHSC Pathology Translational Research Service for assistance with case retrieval and digital slide scanning. They thank the LHSC Neuropathology technologists for assistance with immunostaining.

CONFLICT OF INTEREST
The authors have no conflicts of interests to disclose.

AUTHOR CONTRIBUTIONS
Chelsey ShengQi Zhao, Lee Cyn Ang and Qi Zhang contributed to conception and design of the study; Chelsey ShengQi Zhao, Lei Yan, Wenqing He and Qi Zhang contributed to acquisition and analysis of the data; Chelsey ShengQi Zhao and Qi Zhang contributed to drafting the text or preparing the figures.

ETHICS APPROVAL
This study was approved by the Western University Research Ethics Board (HSREB 113886).

PATIENT CONSENT
All cases were investigated at the London Health Sciences Centre (LHSC) under formal autopsy consent.

DATA AVAILABILITY STATEMENT
The data that support the findings of this study are available from the corresponding author upon reasonable request.

Chelsey ShengQi Zhao[1]
Lei Yan[1]
Wenqing He[2]
Lee Cyn Ang[1,3]
Qi Zhang[1,3]

[1]*Department of Pathology and Laboratory Medicine, Western University, London, Ontario, Canada*
[2]*Department of Statistical and Actuarial Sciences, Western University, London, Ontario, Canada*
[3]*Department of Pathology and Laboratory Medicine, London Health Sciences Centre, London, Ontario, Canada*

Correspondence
Qi Zhang, Department of Pathology and Lab Medicine, London Health Sciences Centre, Western University, 339 Windermere Road, London, ON, Canada, N6A 5A5.
Email: qzhan33@uwo.ca

ORCID
Qi Zhang https://orcid.org/0000-0003-4928-2742

REFERENCES
1. Jabbari E, Holland N, Chelban V, Jones PS, Lamb R, Rawlinson C, et al. Diagnosis across the spectrum of progressive supranuclear palsy and corticobasal syndrome. JAMA Neurol. 2019 Dec 20. Available from: http://www.ncbi.nlm.nih.gov/pubmed/31860007
2. Kovacs GG. Invited review: Neuropathology of tauopathies: principles and practice. Neuropathol Appl Neurobiol. 2015;41(1):3–23.
3. Koga S, Zhou X, Dickson DW. Machine learning-based decision tree classifier for the diagnosis of progressive supranuclear palsy and corticobasal degeneration. Neuropathol Appl Neurobiol. 2021 Apr 7;nan.12710. https://doi.org/10.1111/nan.12710
4. Kovacs GG, Lukic MJ, Irwin DJ, Arzberger T, Respondek G, Lee EB, et al. Distribution patterns of tau pathology in progressive

supranuclear palsy. Acta Neuropathol. 2020;140:99–119. https://doi.org/10.1007/s00401-020-02158-2.
5. Montine TJ, Phelps CH, Beach TG, Bigio EH, Cairns NJ, Dickson DW, et al. National institute on aging-Alzheimer's association guidelines for the neuropathologic assessment of Alzheimer's disease: a practical approach. Acta Neuropathol. 2012;123(1):1–11.
6. Ding JJ, Liu P, Rebernig H, Suller-Marti A, Parrent AG, Burneo JG, et al. Vagus nerve stimulation does not alter brainstem nuclei morphology in refractory epilepsy patients. Epilepsy Behav. 2021;118:107940. https://doi.org/10.1016/j.yebeh.2021.107940
7. Bankhead P, Loughrey MB, Fernández JA, Dombrowski Y, McArt DG, Dunne PD, et al. QuPath: open source software for digital pathology image analysis. Sci Rep. 2017;7(1):1–7.
8. R Core Team. R: A language and environment for statistical computing. 2013. Available from: http://www.r-project.org/
9. Habibzadeh F, Habibzadeh P, Yadollahie M. On determining the most appropriate test cut-off value: the case of tests with continuous results. Biochem Med. 2016;26(3):297–307. https://doi.org/10.11613/BM.2016.034
10. Joutsa J, Horn A, Hsu J, Fox MD. Localizing Parkinsonism based on focal brain lesions. Brain. 2018;(July):1–12. https://doi.org/10.1093/brain/awy161/5047998

SUPPORTING INFORMATION

Additional supporting information may be found in the online version of the article at the publisher's website.

Fig S1

FIGURE S1 Receiver operating characteristic (ROC) graph. ROC curve and area under curve (AUC) values for prediction of PSP

Table S1

TABLE S1 Patient demographic and clinical characteristics (n = 28). NIA-AA: National Institute on Aging–Alzheimer's Association; (A) amyloid plaques Thal score; (B) neurofibrillary tangle Braak score (B); (C) neuritic plaque CERAD score